DEEP-INELASTIC REACTIONS — A NEW TOOL FOR NUCLEAR SPECTROSCOPY*

B. FORNAL[1], R. BRODA[1], W. KRÓLAS[1], T. PAWŁAT[1], P.J. DALY[2]
I.G. BEARDEN[2], Z.W. GRABOWSKI[2], R.H. MAYER[2], D. NISIUS[2]
L. RICHTER[2], M. SFERRAZZA[2], M. CARPENTER[3], R.V.F. JANSSENS[3]
T.L. KHOO[3], T. LAURITSEN[3], D. BAZZACCO[4], S. LUNARDI[4]
C. ROSSI-ALVAREZ[4], G. DE ANGELIS[5], P. BEDNARCZYK[5], H. GRAWE[6]
K.H. MAIER[6] AND R. SCHUBART[6]

[1] H. Niewodniczański Institute of Nuclear Physics
Radzikowskiego 152, 31-342 Kraków, Poland
[2] Chemistry Department, Purdue University
West Lafayette, IN 47907, USA
[3] Argonne National Laboratory
Argonne, IL 60439, USA
[4] Dipartimento di Fisica dell'Universitá di Padova and INFN
I-35131 Padova, Italy
[5] INFN Laboratori Nazionali di Legnaro
I-35020 Legnaro, Italy
[6] Hahn-Meitner-Institut Berlin
D-14109 Berlin, Germany

(Received January 27, 1995)

Binary reaction products of ^{92}Mo+^{60}Ni, ^{106}Cd+^{54}Fe, ^{124}Sn+^{80}Se,^{76}Ge, ^{208}Pb+^{64}Ni and ^{160}Gd+^{36}S, ^{37}Cl heavy ion collisions 10-15% above the barrier have been studied in γ-ray thick target experiments. The product yield distributions have been obtained for some of the reactions from γ-γ coincidence intensities as well as from target radioactivity measurements. The mass transfer between colliding nuclei is discussed in terms of mass and charge equilibration processes. These deep inelastic processes were found to populate a large number of neutron-rich nuclei strongly enough for yrast spectroscopy studies. New spectroscopic results are presented for the *sdf* shell nuclei ^{33}Si, ^{34}P, ^{39}Cl, for ^{64,65,66,67}Ni products and for heavy tin isotopes ^{119,121,122,123,124}Sn. Also yrast excitations in the ^{68}Ni have been identified showing a substantial subshell closure at neutron number $N = 40$.

PACS numbers: 25.70. −z, 25.70. Lm, 23.20. −g, 23.20. Lv

---

* Presented at the XXIX Zakopane School of Physics, Zakopane, Poland, September 5–14, 1994.

1. Introduction

Multinucleon transfer reactions taking place during heavy-ion collisions, with incident energies close to the barrier, produce dozens of excited nuclei around the target and the projectile. Characteristic gamma rays from those products in principle can be measured, but, since the total reaction yield is spread over many nuclei, the spectra are extremely complicated. Development of modern, very efficient Compton suppressed germanium arrays opened new possibilities for studying discrete γ-rays from those heavy ion reaction products.

So far multinucleon transfer reactions have been studied intensively using charged particle spectroscopy which yields valuable information on the reaction kinematics but, on the other hand, suffers from problems in unique identification of charge and mass of the reaction partners. In an approach, in which one forgoes particle detection and uses the γ-γ coincidence method, the precise identification of the two reaction partners and their yields becomes possible. Here, the emission of known gamma-rays identify the final nuclei; an especially important feature is that the coincidences between γ-rays emitted from the reaction partners may be directly observed yielding information on mutual excitation of both reaction fragments.

We have performed several γ–γ coincidence thick target experiments which allowed us to extract a detailed information on the total product yield distribution and the partner–partner correlation in this heavy ion collisions. A brief summary of these reaction related aspects, is given in Section 2. The data were also found to be a source of worthwhile spectroscopic information on the target-like and the projectile-like neutron-rich reaction products. This is the main topic of the present lecture and will be discussed in Section 3.

2. Production yields in heavy ion collisions from γ-ray measurements

2.1. $^{92}Mo+^{60}Ni$ *reaction*

One of the first studies in which the γ–γ coincidences from the binary reaction products were analyzed, was the ^{92}Mo+(255 MeV)^{60}Ni experiment [1]. (The ^{92}Mo target of 0.8 mg/cm^2 thickness with a thick Pb backing to stop both recoils and beam, was used). The experiment had as a main objective the elucidation of high-spin level structures in the fusion-evaporation products ^{149}Ho and ^{150}Er. The excellent γ–γ coincidence data acquired with the Argonne-Notre Dame γ-ray facility (which consisted at that time of eight Compton-suppressed Ge detectors), were found to include many

events arising from inelastic and transfer reaction products. Twelve transfer processes were identified, ranging from $1n$ to $2n2p$ transfer, and involving excitation to moderately high spins up to $I = 12$. The quantitative analysis gave relative cross-sections for various processes involving exchange of particles between the target and projectile, but no clear correlation between the yields and the ground state Q-values was apparent. Mutual excitations of products in the exit channel were observed by detecting γ-rays from one reaction partner in coincidence with gamma transitions from the second product. For example, in the coincidence spectrum gated on the $2^+ \rightarrow 0^+$ transition in ^{56}Fe the γ-rays from the ^{96}Ru reaction partner appeared. Weak γ-rays from ^{95}Ru were also there indicating that evaporation of one neutron took place from the primary products, which could have been either ^{56}Fe+^{96}Ru or ^{57}Fe+^{95}Ru.

In view of all those experimental findings it was apparent that the processes involved in population of the observed γ-decaying states are not of pure quasielastic character.

From a broader viewpoint the results of the Mo+Ni study illustrated the potential of γ–γ coincidence technique for examining some aspects of transfer processes in heavy-ion collisions and, in consequence, the Mo+Ni experiment was followed by a series of similar measurements for several other systems.

2.2. ^{106}Cd+^{54}Fe reaction

In this study the 1.2 mg/cm^2 ^{106}Cd target (backed with Pb) was bombarded with 255 MeV ^{54}Fe beam from the VICKSI accelerator at HMI Berlin [2]. In-beam and off-beam γ-ray coincidence measurements were performed using the OSIRIS multidetector array. Following the in-beam experiment the radioactivity collected in the target was measured and its decay was followed over a period of several months. Very laborious, quantitative analysis of all these data gave production yields for more than 200 nuclei, which is shown in Fig. 1.

The largest cross-sections are grouped in the vicinity of target and projectile; this reflects a contribution from the quasielastic processes. One can note, however, that many nuclei far from the initial masses are still produced with a significant intensity in the deep-inelastic collisions.

Furthermore, from the γ–γ cross-coincidences one concludes that, on the average, excited products in this reaction emit 2.6 nucleons, of which 1.2 are protons. This leads to the important conclusion, that the secondary emission does not affect the N/Z ratio of the primary products. Using the measured yields of all observed isobars, the average N/Z ratio was calculated for each mass. The obtained dependence of the N/Z ratio clearly shows a

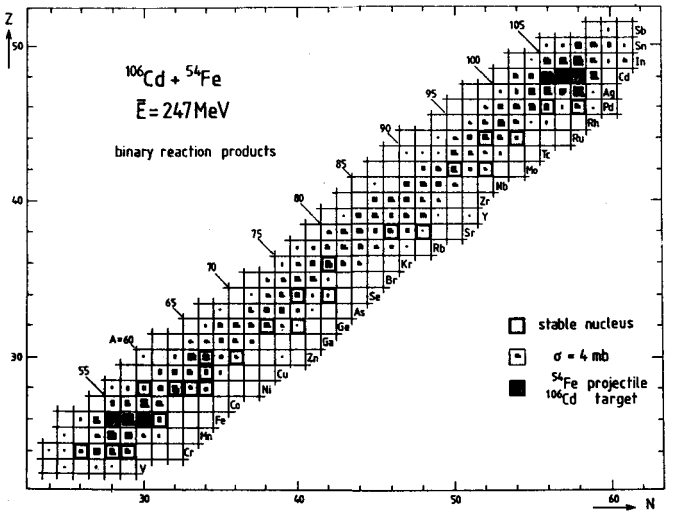

Fig. 1. Production cross sections of binary reaction products for the 247 MeV ^{54}Fe on ^{106}Cd.

trend towards charge equilibration with the number of transferred nucleons and it will be discussed more in Sec. 2.4.

2.3. $^{124}Sn+^{80}Se(^{76}Ge)$ reaction

A series of experiments, which aimed at the yrast spectroscopy studies of heavy tin nuclei, was performed at Argonne National Laboratory [3–7]. Target of ^{124}Sn (backed with Pb) was bombarded with the μs pulsed beams of ^{76}Ge and ^{80}Se (15% above barrier) from the ATLAS accelerator. The in-beam and off-beam γ–γ coincidences were obtained with Argonne-Notre Dame γ-ray facility. A first striking observation was population of the 10^+ seniority isomers in even-even heavy tins in a very broad mass range $A = 116 - 124$ with comparable intensity. This finding prompted us to map the observed distribution of yields with A and Z.

Fig. 2 shows yield determinations of even-even products for the ^{80}Se induced reactions. Also nuclear potential energy contours calculated for the ^{124}Sn+^{80}Se dinuclear system are displayed. A visible shift of the experimental yield distribution towards lighter masses can be attributed to the neutrons evaporated from the excited reaction products. Analysis of the yield distribution gave an estimate of the average number of neutrons evaporated, which then was used to extract the pattern of primary products. This pattern happens to be well correlated with the minimum nuclear potential energy contours and, as a result, it may be broadly understood in

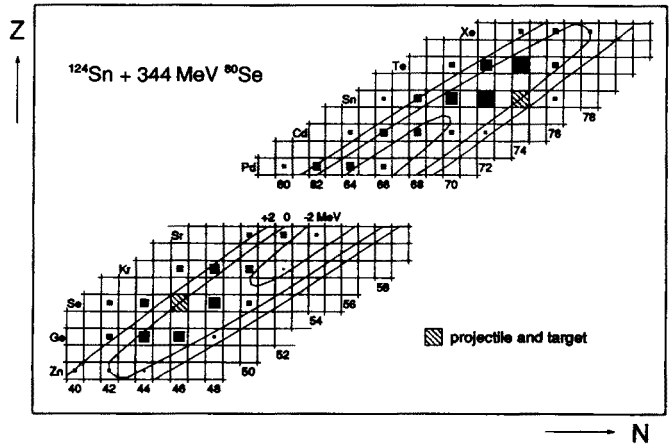

Fig. 2. Relative yields determined for even-even products of the reaction ^{124}Sn+344 MeV ^{80}Se. The nuclear potential energy contours calculated for this dinuclear system are also shown.

terms of the potential energy minimalization of the dinuclear system formed in deep-inelastic collisions.

2.4. $^{208}Pb+^{64}Ni$ reaction

Another thick target γ–γ coincidence experiment was performed for the ^{208}Pb+350MeV ^{64}Ni system with the OSIRIS array at the HMI Berlin. At that beam energy (11% above Coulomb barrier) deep-inelastic processes contribute predominantly to the reaction cross-section. The spectroscopy of ^{207}Pb [8] and ^{208}Pb [9] was an interesting result obtained from that experiment; in parallel, the reaction aspects were analyzed with partial results published in [10, 11]. From the analysis of the in-beam and off-beam coincidence data as well as from the detailed radioactivity measurement, nearly complete distribution of product yields was obtained for nuclei produced in the range $Z = 22 - 87$. This distribution is shown in Fig. 3. Here again the largest cross sections are found in the neighbourhood of target and projectile — this is due to quasielastic processes. Production of nuclei far away from initial masses also takes place with appreciable intensity. The measured distribution, however, is a distribution of the secondary products, which arise after evaporation of neutrons from the excited primary products. The completeness of the experimental data in this case allowed us to make an attempt to reconstruct the distribution of primary fragments. The method is based on the fact that all binary reaction products for the ^{208}Pb+^{64}Ni system are rather neutron-rich and evaporate mostly neutrons. As a result for each pair of complementary elements produced

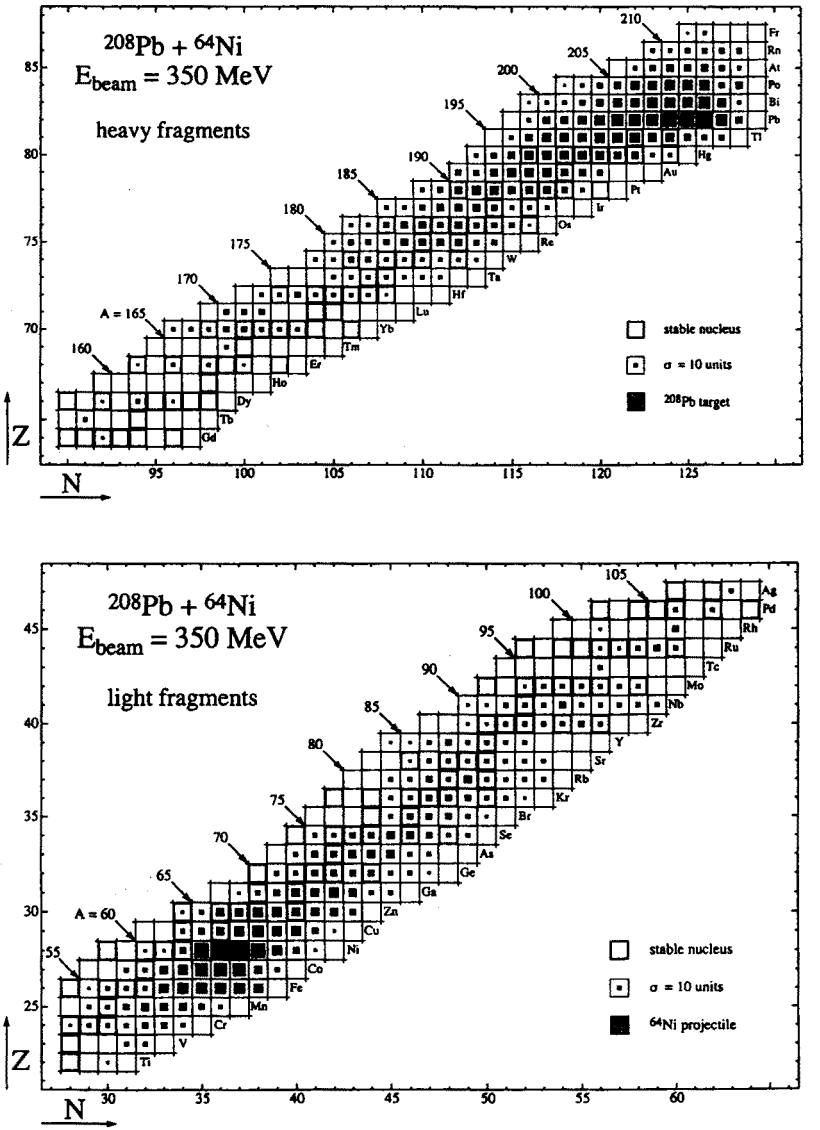

Fig. 3. Distribution of relative product yields for the ^{208}Pb+350 MeV ^{64}Ni reaction.

Z_1, Z_2 ($Z_1 + Z_2 = 110$) one can establish an average number of missing neutrons $\langle \Delta N \rangle_{Z_1 Z_2} = 162 - \langle N \rangle_{Z_1} - \langle N \rangle_{Z_2}$, where $\langle N \rangle_{Z_1}$, $\langle N \rangle_{Z_2}$ are the weighted average neutron numbers for Z_1 and Z_2 complementary products, respectively. Assuming excitation energy division proportional to the product masses $\langle M_{Z_1} \rangle$, $\langle M_{Z_2} \rangle$, the missing neutron number $\Delta N_{Z_1 Z_2}$ was then

used for calculating ΔN_{Z_1} and ΔN_{Z_2} — numbers of neutrons evaporated from the Z_1 and Z_2 products. The primary product distribution was obtained by shifting the Z_1, Z_2 distributions by ΔN_{Z_1} and ΔN_{Z_2}, respectively, and repeating this procedure for each product pair Z_1, Z_2. The weighted N/Z ratio for each primary product mass could then be extracted.

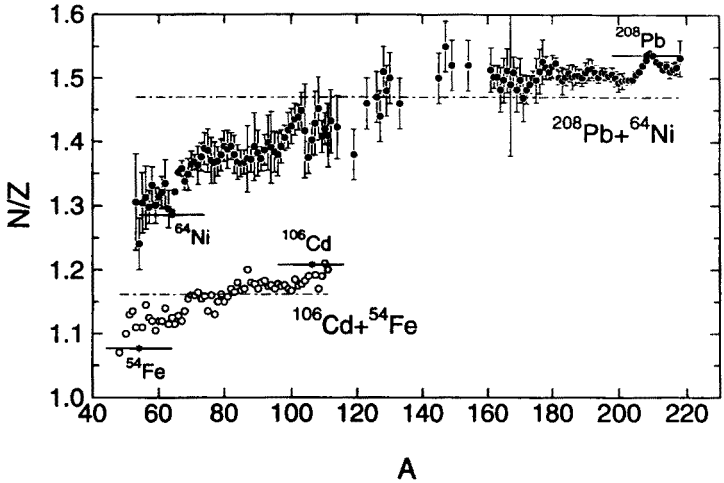

Fig. 4. Average N/Z ratio for primary products (see text) for ^{208}Pb+^{64}Ni and ^{106}Cd+^{54}Fe systems.

Fig. 4 shows the N/Z ratio as a function of the product mass for the ^{106}Cd+^{54}Fe and ^{208}Pb+^{64}Ni systems. Almost all points fall into the limits given by the N/Z of the target and the projectile. In both cases the N/Z ratio evolves towards that of the composite system, as the mass transfer increases. Trend is similar in both reactions despite the fact that the Pb+Ni system spans a much broader N/Z range than the Cd+Fe combination.

3. Spectroscopic results

Already the overall results of the Mo+Ni study, discussed partially in Sec. 2.1, indicated that γ–γ technique might have potential for exploring the yrast spectroscopy of certain neutron excessive nuclei that are inaccessible by fusion-evaporation reactions. Indeed, all studied reactions, discussed in Section 2, yielded new spectroscopic findings. In addition, some of the existing high quality γ–γ coincidence data were reanalyzed to get new information on spectroscopy of the deep-inelastic products.

3.1. Neutron-rich sdf shell nuclei

We have performed detailed analysis of low multiplicity subsets of the γ–γ coincidence data for reactions of ^{34}S, ^{36}S and ^{37}Cl beams on thick ^{160}Gd targets, which originally were used for superdeformed band studies in nuclei of the $A \sim 190$ region at Argonne National Laboratory [12]. The favored processes were those involving addition of protons to the ^{160}Gd target (with or without neutron transfer) or removal of neutrons from ^{160}Gd thus leading to neutron rich nuclei around ^{36}S and ^{37}Cl. In the two neutron transfer products ^{38}S and ^{39}Cl, yrast states were populated with the highest intensity. Cascades deexciting known states up to $I \sim 6$ were observed in those nuclei. For the ^{39}Cl nucleus it was possible to locate a new yrast level at 3520 keV tentatively assigned as $15/2^+$ — the highest member of the $\pi d_{3/2}(\nu f_{7/2})^2$ multiplet, decaying to the $(11/2)^+$ level at 2835 keV.

The γ-rays deexciting known yrast states up to $I \sim 6$ in the $N = 20$ products ^{34}Si, ^{35}P, ^{36}S and ^{37}Cl were also observed in these reactions.

The present studies yielded some information about the spectroscopy of ^{33}Si and ^{34}P, which were very poorly known. The ^{34}P nucleus was a product of the $2p1n$ transfer in the ^{37}Cl induced reaction. The 429.1 keV ground transition, known from ^{34}Si β-decay studies, appeared in coincidence with the 1876 keV γ-ray. Both transitions are placed in the ^{34}P level scheme shown in Fig. 5. The 429 and 1876 keV lines were observed also in cross coincidences with γ-rays from the partner ^{162}Dy–$2p$ transfer product. The identification in the ^{160}Gd+^{37}Cl reaction of ^{34}P γ-rays in coincidence with these of ^{162}Dy implies that a neutron was evaporated from one of the primary products which could have been either ^{34}P+^{163}Dy or ^{35}P+^{162}Dy.

In ^{34}P, the 1^+ ground state and 429 keV 2^+ state are assigned to the $\pi s_{1/2}\nu d_{3/2}$ configuration. The 2305 keV level located in the present work is a very good candidate for the next yrast state of the type $\pi s_{1/2}\nu f_{7/2}$ with $I^\pi = 3^-$ or 4^-.

The simultaneous production of ^{34}P and ^{162}Dy described above for the ^{160}Gd+^{37}Cl reaction suggested that in the ^{36}S induced reaction one might similarly observe coincidences between ^{33}Si and ^{162}Dy γ-rays. Inspection of the appropriate γ-ray coincidence spectrum gated on ^{162}Dy lines revealed, in addition to the ^{34}Si transitions, a single strong 1435 keV γ-ray that was interpreted as a ground state transition in ^{33}Si, deexciting the $(7/2^-)$ level — Fig. 5. A second much weaker 1010 keV γ-ray is also tentatively placed in the ^{33}Si scheme.

It is worthwhile to emphasize that all these results, although rather fragmentary and scattered, concern the *sdf* shell nuclei, which are very difficult to produce in any other way, but are extremely important for complete theoretical shell model calculations.

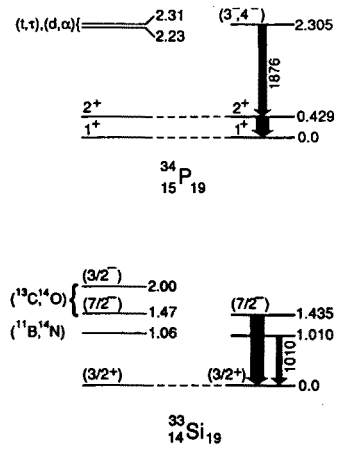

Fig. 5. Proposed decay schemes for ^{34}P and ^{33}Si. The arrow widths denote relative γ-ray coincidence intensities observed with gates on transitions in the reaction partner. Levels located previously in the specified transfer reactions are shown on the left.

3.2. Neutron-rich Ni isotopes

The ^{208}Pb+^{64}Ni experiment, which yielded very extensive data on production yields, discussed in Sec. 2.4, was a source of the worthwhile information on neutron-rich Ni isotopes [13].

In the closed $Z = 28$ proton shell Ni nuclei the neutron Fermi level is located within the $p_{3/2}$, $f_{5/2}$ and $p_{1/2}$ orbitals and with increasing neutron number it moves towards the $g_{9/2}$ orbital. In heavier Ni isotopes this j positive $g_{9/2}$ neutron level is expected to play a crucial role in yrast excitations.

Fig. 6 displays the level schemes of ^{64,65,66,67}Ni isotopes which until now could not be reached in processes suitable for γ-spectroscopy. They include all excitations observed in the present work. In ^{64}Ni only five and in ^{66}Ni only three low lying γ-transitions have been observed previously. Particularly interesting are the $\nu g_{9/2}^2$ 8^+ and $\nu g_{9/2} f_{5/2}^{-1}$ 7^- high spin states revealed earlier by the $(\alpha, 2p)$ study in both, ^{64}Ni and ^{66}Ni nuclei. Their exact energies and γ-decay are now established.

Considering the two transitions connecting the 7^- and the $g_{9/2}p_{1/2}$ 5^- yrast states, we tentatively assign the $g_{9/2} f_{5/2}^{-1}$ 6^- to the intermediate state. In the ^{66}Ni it becomes isomeric reflecting the forbidden character of the $M1$ $f_{5/2}^{-1} \rightarrow p_{1/2}$ transition.

The level schemes for odd ^{65}Ni and ^{67}Ni nuclei represent excitations observed in $1n$ and $3n$ transfer. Of special interest is the identification of the 1017 keV $g_{9/2}$ 25 ns isomer in the ^{65}Ni product.

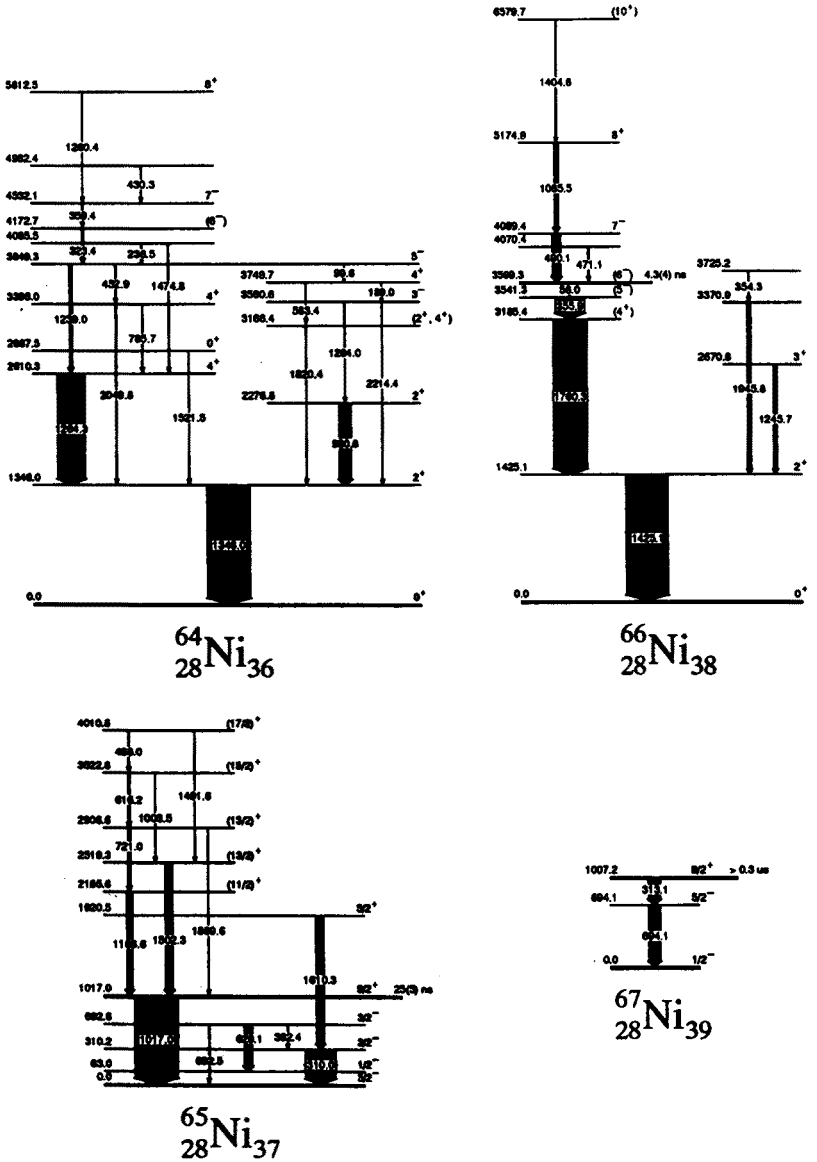

Fig. 6. Level schemes of the ^{64,65,66,67}Ni nuclei deduced from the ^{208}Pb+^{64}Ni γ–γ coincidence experiment.

In the ^{67}Ni nucleus the $1/2^-$ g.s. and 694 keV $5/2^-$ states were known from the radioactive decay data. For the observed long lived isomer decaying via 313–694 keV cascade, the intensity and systematics expectations strongly suggest a $\nu g_{9/2}$ nature. We were able to give only the lower limit 0.3μs on its half-life; the value deduced from the corresponding transitions in ^{63}Ni and ^{65}Ni is about 10μs.

3.3. Seniority isomers in heavy tins

The neutron $h_{11/2}$ subshell is being filled in the $A = 116 - 130$ tin isotopes. From previous works the $(\nu h_{11/2})^n$ 10^+ isomers were known in ^{116,118,120}Sn at one end, and in the fission products ^{128,130}Sn at the other. Missing was information on the ^{122,124,126}Sn isotopes — these nuclei cannot be made by fusion-evaporation.

In the experiment mentioned in Sec. 2.3, in which the ^{124}Sn target was bombarded with ^{76}Ge and ^{80}Se beams, we managed to identify the 10^+ isomers in ^{122}Sn and ^{124}Sn (but not ^{126}Sn) among the products of heavy ion collisions [3, 4]. The cascades $10^+ \rightarrow 8^+ \rightarrow 7^-$ were clearly seen and the half-lives of the 10^+ states were measured yielding 62μs and 45μs in ^{122}Sn and ^{124}Sn, respectively. These results almost completed a series of $B(E2)$ determinations for $(\nu h_{11/2})^n$ states in even A $^{116-130}$Sn isotopes.

In odd tins with $A = 119, 121$ and 123, which were found to be produced in present reaction, new γ-cascades deexciting microsecond $19/2^+$ isomers have been identified [5, 6]. These states are of the $(\nu h^2_{11/2} s_{1/2})$ $19/2^+$ character and decay only by configuration forbidden M2 transitions to the $15/2^-$ states. The identification of the $15/2^- \rightarrow 11/2^-$ transitions in ^{119,121,123}Sn was a significant step towards further studies of $(\nu h_{11/2})^n$ $\nu = 3$ yrast states in those nuclei. For example, by setting coincidence gates on these lowest transitions, γ-ray cascades 175–513–1105 keV in ^{119}Sn and 176–471–1030 keV in ^{121}Sn could be firmly established as $27/2^- \rightarrow 23/2^- \rightarrow 19/2^- \rightarrow 15/2^-$ transitions between $(\nu h_{11/2})^n$ $\nu = 3$ states in these two nuclei. Half-lives for the $27/2^-$ isomers in ^{119,121}Sn were determined from the ^{124}Sn+^{80}Se data [7] and are shown in Fig. 7.

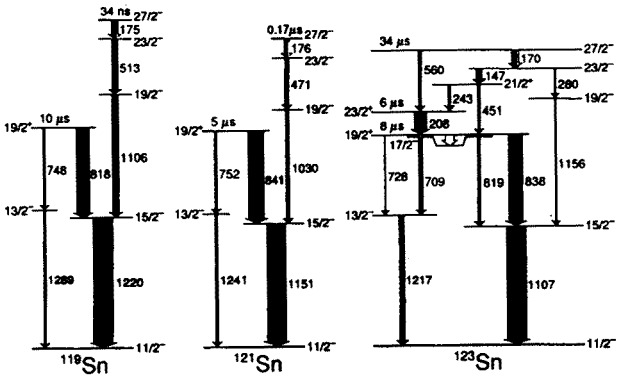

Fig. 7. Isomeric decay schemes for ^{119}Sn, ^{121}Sn and ^{123}Sn. Widths of transitions are proportional to the observed intensities.

In the follow-up experiment we extended the ATLAS investigations by studying the system ^{124}Sn+655 MeV ^{136}Xe. We expected on the basis of N/Z equilibration considerations that the ^{136}Xe beam would favor production of neutron-rich nuclei more than the ^{76}Ge and ^{80}Se beams. Indeed, the overall experimental yield distribution in the $Z = 50$ region was definitely shifted towards higher neutron numbers. Very important in the present situation were the high quality prompt and delayed γ-ray coincidence data obtained for ^{123}Sn. In coincidence with the 1107 keV $15/2^- \rightarrow 11/2^-$ ^{123}Sn transition, γ-cascades crossing the microsecond intermediate isomers as well as prompt γ-rays, established a very complete ^{123}Sn level scheme up to a 34μs isomeric level at 2713 keV — Fig. 7.

This isomer and the level at 2543 keV are, without doubt, the $(\nu h_{11/2})^n$ $\nu = 3$ $27/2^-$ and $23/2^-$ states. Very low value of the $B(E2, 27/2^- \rightarrow 23/2^-, {}^{123}\mathrm{Sn})$ equals to $0.06e^2\mathrm{fm}^2$ (less than 2×10^{-3} W.u.) reflects the half-filling of the $\nu h_{11/2}$ subshell at $N = 73$, and is a striking illustration of the impact of subshell occupation on transition probabilities.

For the isomeric transitions between $(\nu h_{11/2})^n$ states in the tin isotopes the dependence of the $E2$ transition probability is proportional to the $(6-n)^2$ where n is the $\nu h_{11/2}$ subshell occupation number. It is convenient to plot the $E2$ transition amplitude (or square roots of the measured $B(E2)$ values) *versus* A, knowing that the $E2$ matrix element must have opposite signs in the bottom and top halves of the $\nu h_{11/2}$ subshell. All the $E2$ amplitudes determined for the Sn isotopes are displayed in Fig. 8 (the $\sqrt{B(E2)}$ values for the odd-A nuclei were multiplied by a constant to compensate for geometrical factor entering the $\nu = 2$ and $\nu = 3$ $B(E2)$ equations). The results for the odd-A nuclei match very nicely with those for the even-A tin isotopes reinforcing conclusions about the $\nu h_{11/2}$ subshell filling.

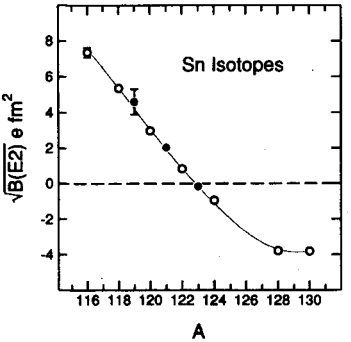

Fig. 8. $E2$ transitions amplitudes for $(\nu h_{11/2})^n$ $10^+ \rightarrow 8^+$ and $27/2^- \rightarrow 23/2^-$ transitions in even-A and odd-A Sn isotopes (values for the odd-A nuclei have been multiplied by a factor 0.514 to put them on the same, as even-A ones, scale).

3.4. Neutron subshell closure in the ^{68}Ni

The ^{68}Ni nucleus with the $N = 40$ neutron number and closed proton shell is expected to exhibit a double shell closure features as it is for the ^{90}Zr nucleus with $N = 50$ and $Z = 40$. Lying on the neutron-rich side of the stability line it could not be accessed by fusion-evaporation reactions. In fact, the only known excitation in ^{68}Ni, a 0^+ state at 1.77 MeV, was located using the ^{70}Zn(^{14}C,^{16}O) two-proton transfer reaction.

In the experiment ^{208}Pb+^{64}Ni, which yielded new spectroscopic findings on ^{64,65,66,67}Ni nuclei (Sec. 3.3) the production of ^{68}Ni was clearly indicated but no γ-ray could be identified with this isotope because of the insufficient statistics. To improve the experimental conditions we performed at the INFN Legnaro a similar measurement for the ^{130}Te +^{64}Ni system using the much more powerful GASP multidetector array. The 275 MeV ^{64}Ni beam was used on a 1.2 mg/cm^2 ^{130}Te target on a 14 mg/cm^2 ^{208}Pb backing.

The ^{68}Ni level spectrum, like that of ^{90}Zr, should exhibit a long-lived 5^- isomer as well as a significant increase of the 2^+ excitation energy with respect to the lighter Ni isotopes. Examination of the expected energy region of the off-beam γ–γ coincidence data, revealed two coincident 814 keV and 2033 keV transitions — very good candidates for the $5^- \rightarrow 2^+ \rightarrow 0^+$ yrast cascade in ^{68}Ni. Both transitions appeared in the ^{208}Pb and ^{130}Te target experiments with intensities consistent with the production yields of the ^{68}Ni isotope.

The isotopic identification was performed using the γ–γ cross-coincidences of the superior quality GASP data for the ^{130}Te+^{64}Ni system. The results are presented in Fig. 9. When a gate was set on a strong transition of a specific Ni product, the coincidence spectrum showed, in addition to other γ-rays of that Ni nucleus, also known γ-rays from various Te partner nuclei produced simultaneously in the exit channel. Approximate yields of the Te products could be estimated from the coincident γ-ray intensities.

Starting from the top of Fig. 9, the tellurium isotope yields in coincidence with the ^{64}Ni 1346 keV γ-ray show that ^{64}Ni appears in the exit channel accompanied by tellurium partners with $A = 126 - 130$, produced in processes involving 0–4 neutron evaporation. For heavier Ni isotopes the pattern of tellurium reaction partners shifts towards lighter mass with sharp cut-off at the high mass corresponding to the $A = 194$ total mass of the system. For ^{68}Ni (at the bottom) the events giving rise to cross-coincidences were only those, in which prompt population of the presumed 2033 2^+ state takes place. Nevertheless, the excellent statistics of the GASP data allowed us to observe prompt coincidences between the 2033 keV line and transition of the Te isotopes with $A = 126 - 122$-products of a transfer of at least four neutrons to the ^{64}Ni projectile and subsequent evaporation of zero to

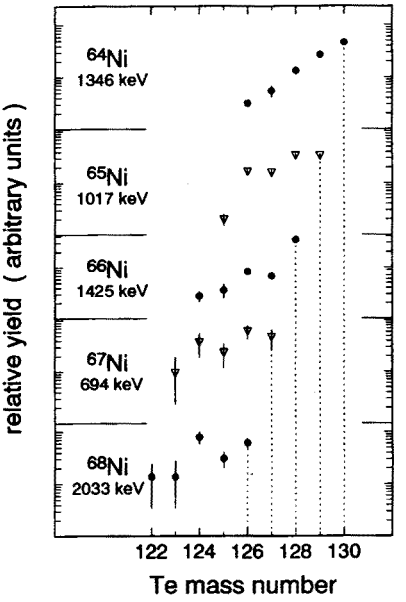

Fig. 9. Yields of Te partner isotopes from intensities of γ cross coincidences with the indicated γ lines of Ni products. The vertical lines mark the limits defined by the $A = 194$ total mass of the system.

four neutrons from the primary products. The above results establishes the assignment of the 2033 keV transition to the ^{68}Ni and the ordering 813–2033 keV in the isomeric decay cascade assigned in analogy to ^{90}Zr as $5^- \rightarrow 2^+ \rightarrow 0^+$ cascade.

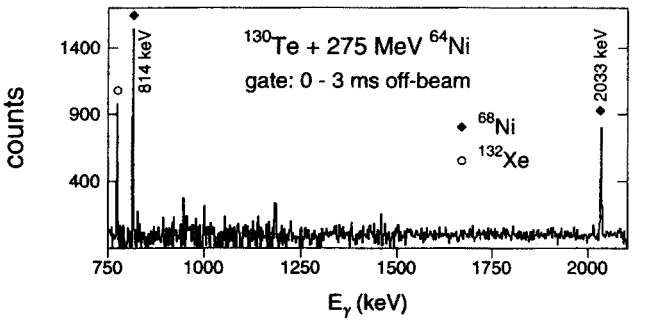

Fig. 10. Part of the off-beam single γ-spectrum, taken in the time range enhancing the ^{68}Ni isomer decay (radioactivity background subtracted).

In order to confirm this assignment we performed a separate experiment to measure the half-life of the isomer again with the GASP array and using the same reaction. The beam was pulsed in the range of micro- and millisec-

onds. The γ–γ coincidences as well as singles from all detectors were stored as a function of time. For the main run used for the half-life determination the beam pulsing conditions 3 ms-on and 10 ms-off were used. The off-beam spectrum enhancing the $5^- \rightarrow 2^+ \rightarrow 0^+$ ^{68}Ni isomeric cascade is shown in Fig. 10. Both transitions 814 and 2033 keV showed the same intensity and the same decay. The weighted average gave the half-life of $T_{1/2} = 0.86(5)$ms [14].

The prompt coincidence spectrum taken with the 2033 keV gate, showed the 1114 keV line in both, the ^{208}Pb and ^{130}Te target experiments; it is much weaker than the 814 keV isomeric transition but clearly belong to the nucleus. It establishes another state in ^{68}Ni above the 5^- isomer, From considerations based on systematics we assign tentatively this state as the 4^+ excitation, although the 3^- assignment is also possible.

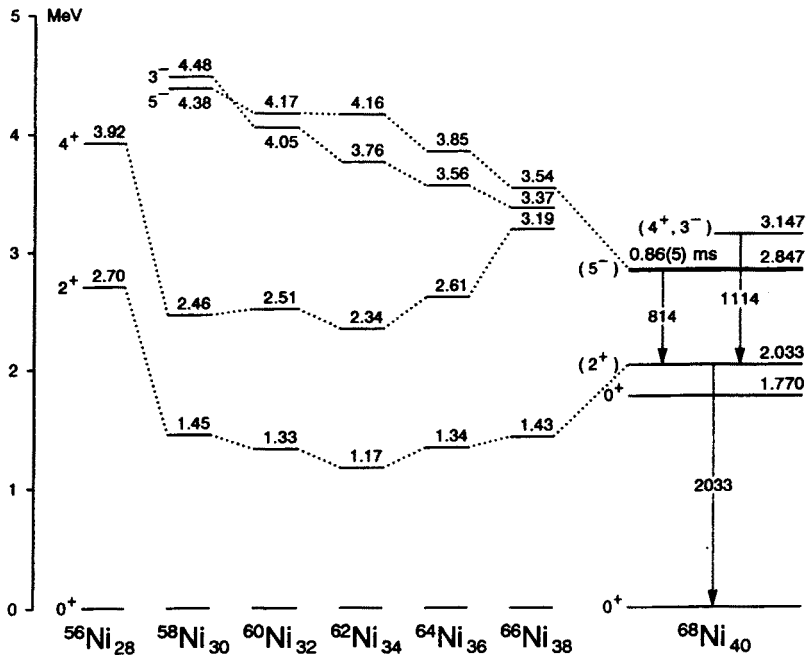

Fig. 11. Systematics of selected states in even Ni isotopes. The ^{68}Ni results are outlined.

In Fig. 11 the systematics of the lowest excited states in even nickel isotopes is displayed together with the new findings in ^{68}Ni.

Our results indicate a significant subshell closure at the $N = 40$ neutron number. Future experiments are now planned aiming at search for higher lying states in ^{68}Ni and at identification of excitations in the ^{70}Ni isotope.

4. Conclusions

In summary, the thick target measurements of γ-rays from the binary heavy ion reaction products proof to be a powerful method for studying yrast states in some neutron-rich nuclei, which are inaccessible otherwise. The results illustrate also that the γ–γ coincidence technique can be used to examine at high resolution some aspects of multinucleon transfer processes, such as the mass flow between projectile and target or energy and angular momentum transfer into product nuclei. These studies will benefit considerably from the enhanced sensitivity of the new, large γ-ray detector arrays, which are coming into operation at the laboratories, where a broad variety of heavy-ion beams is available.

This work has been supported by the Polish Scientific Committee under grant no. 224319203, by the U.S. Department of Energy under contracts DE-FG02-87ER40346 and W-31-109-ENG-38, by the German–Polish collaboration (project X081.51) and by the Italian–Polish collaboration.

REFERENCES

[1] R. Broda, M.A. Quader, P.J. Daly, R.V.F. Janssens, T.L. Khoo, W.C. Ma, M.W. Drigert, *Phys. Lett.* **B251**, 245 (1990).

[2] B. Broda, C.T. Zhang, P. Kleinheinz, R. Menegazzo, K.H.Maier, H.Grawe, M.Schramm, R.Schubart, M. Lach, S. Hofmann, *Phys. Rev.* **C49**, R575 (1994).

[3] R. Broda, R.H. Mayer, I.G. Bearden, Ph. Benet, P.J. Daly, Z.W. Grabowski, M.P. Carpenter, R.V.F. Janssens, T.L. Khoo, T. Lauritsen, E.F. Moore, S. Lunardi, J. Blomqvist, *Phys. Rev. Lett.* **68**, 1671 (1992).

[4] R. Broda, Proc. of the 22nd Masurian Lakes Summer School on Nuclear Physics, Poland, August 26-September 5, 1991, p. 139.

[5] P. Daly, R. Broda, B. Fornal, R.H. Mayer, D. Nisius, I. Bearden, Ph. Benet, Z.W. Grabowski, T. Lauritsen, M. Carpenter, R.V.F. Janssens, T.L. Khoo, Y. Liang, S. Lunardi, J. Blomqvist, Proc. of the 4th International Spring Seminar on Nuclear Physics, Amalfi, Italy, May 18-22, 1992.

[6] R.H. Mayer, B. Fornal, R. Broda, I.G. Bearden, Z.W. Grabowski, S. Lunardi, P.J. Daly, T. Lauritsen, M.P. Carpenter, R.V.F. Janssens, T.L. Khoo, Y. Liang, *Z. Phys.* **A342**, 247 (1992).

[7] R.H. Mayer, D. Nisius, I.G. Bearden, P. Bhattacharyya, L. Richter, M. Sferrazza, Z.W. Grabowski, P.J. Daly, R. Broda, B. Fornal, I. Ahmad, M.P. Carpenter, R.G. Henry, R.V.F. Janssens, T.L. Khoo, T. Lauritsen, Y. Liang, J. Blomqvist, *Phys. Lett.* **B336**, 308 (1994).

[8] M. Schramm, H. Grawe, J. Heese, H. Kluge, K.H. Maier, R. Schubart, R. Broda, J. Grębosz, W. Królas, A. Maj, J. Blomqvist, *Z. Phys.* **A344**, 121 (1992).

[9] M. Schramm, H. Grawe, J. Heese, H. Kluge, K.H. Maier, R. Schubart, R. Broda, J. Grębosz, W. Królas, A. Maj, J. Blomqvist, *Z. Phys.* **A344**, 363 (1993).

[10] W. Królas, R. Broda, J. Grębosz, A. Maj, T. Pawłat, M. Schramm, H. Grawe, J. Heese, H. Kluge, K.H. Maier, R. Schubart, *Acta Phys. Pol.* **B24**, 449 (1993).

[11] W. Królas, R. Broda, J. Grębosz, A. Maj, T. Pawłat, M. Schramm, H. Grawe, J. Heese, H. Kluge, K.H. Maier, R. Schubart, *Acta Phys. Pol.* **B25**, 687 (1994).

[12] B. Fornal, R.H. Mayer, I.G. Bearden, Ph. Benet, R. Broda, P.J. Daly, Z.W. Grabowski, I. Ahmad, M.P. Carpenter, P.B. Fernandez, R.V.F. Janssens, T.L. Khoo, L. Lauritsen, E.F. Moore, M. Drigert, *Phys. Rev.* **C49**, 2413 (1994).

[13] T. Pawłat, R. Broda, W. Królas, A. Maj, M. Ziębliński, H. Grawe, R. Schubart, K.H. Maier, J. Heese, H. Kluge, M. Schramm, *Nucl. Phys.* **A574**, 623 (1994).

[14] R. Broda, B. Fornal, W. Królas, T. Pawłat, D. Bazzacco, S. Lunardi, C. Rossi-Alvarez, R. Menegazzo, G. de Angelis, P. Bednarczyk, J. Rico, D. De Acuna, P.J. Daly, R.H. Mayer, M. Sferrazza, H. Grawe, K.H. Maier, R. Schubart, *Phys. Rev. Lett.* (in press).